Paste 2026 – AB Fourie, M Horta, M Oliveira & S Wilson (eds)

doi:10.36487/ACG_repo/2655_50

A fluid–structure interaction study of upset load from material build-up in raked thickeners

Yaojun Lu [a,*], Thien Sok [a], Jeremy Scott [a], Craig Gilbert [a]

[a] *FLSmidth, USA*

Abstract

Raked thickeners are critical to mineral processing, yet their design often relies on empirical correlations that fail to predict transient upset loads, leading to over-design or catastrophic mechanical failures. This study presents a high-fidelity, one-way fluid–structure interaction (FSI) framework to quantify transient rake loads induced by extreme material accumulation (island formation) on the floor of a 45 m industrial deep-cone thickener. Transient computational fluid dynamics (CFD) simulations were utilised to model non-Newtonian slurry dynamics and map hydraulic pressure and shear-stress distributions directly onto a finite element analysis (FEA) structural model. Two worst-case upset scenarios were evaluated: an inner island engaged by both short and long rake arms, and an outer island engaged exclusively by the long arm. Results demonstrate that outer island formation induces up to an 88% increase in rotational torque and a 593% increase in non-rotational forces compared to normal steady-state operation. Despite peak rotational torques reaching 366,951 N·m, structural stresses remained below 66 MPa, well within the yield limits of standard structural steels. The findings highlight that while island-induced loads do not immediately threaten structural integrity, the resulting asymmetric forces and severe torque spikes are critical sizing parameters for drive systems and operational control strategies.

Keywords: *raked thickener, mineral processing, normal load, upset load, fluid–structure interaction*

1 Introduction

Raked thickeners serve as the primary solid–liquid separation stage in mineral processing circuits, crucial for tailings disposal and water recovery. The rake mechanism within these thickeners plays a pivotal role in maintaining operational stability and achieving target underflow densities. More specifically, the rake performs 2 essential functions: it mobilises and transports flocculated/settled solids from the mud-bed to the underflow discharge zone, and it promotes dewatering of the consolidated sediment by gently disturbing the bed, thereby enhancing water release and compaction. A well-designed rake system ensures consistent thickening performance and underflow quality, which is critical for downstream processing efficiency and water balance.

Despite its importance, the raking process in thickeners remains poorly understood, particularly under full-scale industrial conditions. Much of the existing research has focused on clarifiers used in municipal and industrial waste water treatment (Warden 1981; Gunthert 1984; Albertson & Okey 1992; Frost et al. 1993), or on laboratory-scale studies of mineral thickeners (Rudman et al. 2008, 2010; Sutalo et al. 2003). However, these studies often involve different fluid properties, tank geometries, and operational regimes, making direct application to industrial paste thickeners problematic. Additionally, scale effects – such as increased rake arm length, elevated and non-uniform solids loading, and non-Newtonian slurry behaviour – further complicate the extrapolation of small-scale findings to full-scale design. In smaller pilot units, the rake mechanism naturally produces a higher number of materials passes per unit bed volume, enhancing bed conditioning and reducing localised channelling. When scaling up, this effective rake coverage is maintained

[*] Corresponding author. Email address: yaojunlu@flowsepdynamics.com

through rake geometry and consistent engagement with the active compression zone rather than by increasing rotational speed. As a result, rake tip speeds remain relatively low to minimise floc degradation and shear while still ensuring adequate rake passes to support stable consolidation and underflow performance.

In practice, rake sizing and drive capacity are frequently determined using empirical correlations, bench-top tests, or simplified raked cylinder experiments. While these methods offer convenience, they often lack the resolution and fidelity needed to capture transient and localised loading phenomena. As a result, rake systems may be under-designed, leading to torque spikes, rat-holing, and rake blockage, or over-designed, resulting in unnecessary capital and energy costs. These design deficiencies can compromise thickener performance, reduce equipment life, and contribute to inconsistent underflow quality.

To overcome these limitations, a high-fidelity fluid–structure interaction (FSI) approach was recently developed for predicting rake loads under normal operating conditions in a full-scale thickener (Lu et al. 2024). This methodology couples transient computational fluid dynamics (CFD) simulations with finite element analysis (FEA), enabling detailed quantification of hydraulic loads and structural responses. The CFD model captures the complex mud-rake interactions, including feed conditions, slurry rheology, and mud-bed geometry, while the FEA model evaluates deformation and stress under realistic loading scenarios.

Building on this foundation, the present study extends the FSI framework to evaluate upset loads – those arising under exceptional conditions such as thick material accumulation or island formation on the thickener floor. Two scenarios are analysed: inner island formation within the short-arm reach, and outer island formation beyond it, where only the long arm engages the material. By mapping CFD-derived pressure and shear-stress into the FEA model, the study achieves seamless load transition and realistic structural assessment.

The proposed FSI methodology provides a robust and scalable framework for optimising rake design. It supports both the sizing of new thickeners and the troubleshooting of existing installations – especially in high-density paste environments where conventional design methods often prove inadequate. By enabling data-driven insights, this approach enhances operational resilience and promotes more efficient thickener performance.

2 Rake loads

In industrial thickeners, rake mechanisms are designated to deliver high torque at low rotational speeds, typically powered by central or peripheral drive systems. Depending on the thickener's type and configuration, rakes may be suspended from overhead bridges or supported by central columns. While their mechanical design varies, all rake systems are tasked with maintaining bed mobility and preventing solids accumulation that could compromise thickener performance. Although modern installations incorporate torque monitoring and overload protection systems, field operations continue to report persistent challenges – including torque spikes, rake blockage, rat-holing, and inconsistent underflow density. These issues often arise from transient or localised loading events that exceed design specifications, particularly during upset conditions such as island formation or feed surges. Such occurrences highlight the limitations of conventional design practices and the need for more accurate load quantification methods. From a design and operational standpoint, rake loads can be broadly classified into 2 categories: normal loads and upset loads.

2.1 Normal loads

Normal rake loads refer to the mechanical forces and torques encountered during steady-state operation, where the rake system interacts with a uniformly settled mud bed. These loads are primarily governed by viscous shear stresses and pressure gradients acting on the rake blades and arm surfaces as they rotate at a designated speed. To maintain continuous solids transport and bed mobility, the rake must overcome the cohesive structure and yield stress of the sediment. The magnitude of these loads is directly influenced by the rheological properties of the slurry – namely, its viscosity, density, and yield stress.

In practice, normal rake loads are closely tied to energy consumption, drive system sizing, and long-term operational costs. They serve as a baseline for mechanical design, performance benchmarking, and predictive maintenance planning. However, the evolution of thickener technology over the past century has significantly reshaped the landscape of rake loading.

Early conventional thickeners, such as those described by Hazen (1904), operated at low solids concentrations and shallow feedwell configurations, resulting in relatively modest rake loads. Subsequent advancements introduced high-rate thickeners with flocculated feed and improved settling kinetics (McCarty & Olson 1959), followed by paste thickeners designed to produce elevated underflow densities (Gollaher et al. 2010). More recently, deep-cone thickeners have emerged, characterised by steep floor angles and deep mud beds that impose substantially higher mechanical demands on the rake systems.

Modern high-density thickeners routinely generate underflows with apparent yield stresses ranging from 30–100 Pa, while deep-cone configurations often exceed 100 Pa (Schoenbrunn 2011). In contrast, conventional and high-rate thickeners typically operate within a yield stress range of 20–30 Pa. As underflow density increases, the slurry's resistance to deformation rises – often nonlinearly – resulting in elevated normal rake loads. This effect becomes particularly pronounced when solids concentration surpasses a critical threshold, beyond which the mud bed exhibits viscoplastic behaviour and resists shear more aggressively.

These elevated loads necessitate more robust rake structures and drive assemblies capable of withstanding intensified mechanical stresses. Design considerations must extend beyond torque capacity to include structural deflection, fatigue resistance, and long-term wear. Material selection, blade geometry, and arm configuration all play critical roles in optimising rake performance under demanding conditions. An accurate quantification of normal rake loads is therefore essential for ensuring reliable operation, minimising downtime, and achieving consistent underflow quality in modern thickener installations.

2.2 Upset loads

Beyond steady-state operation, thickener rakes may be subjected to upset loads – transient, high-magnitude forces and torques triggered by exceptional process conditions. These events typically arise from localised accumulations of dense solids on the thickener floor, forming sediment islands or obstructive deposits that exceed the rake's designed clearance envelope and torque capacity. If not promptly mitigated, such anomalies can cause severe operational disruptions, including thick bed-material build-up as shown in Figure 1, drive system overload, rake arm blockage, and in extreme cases, structural failure of rake components.

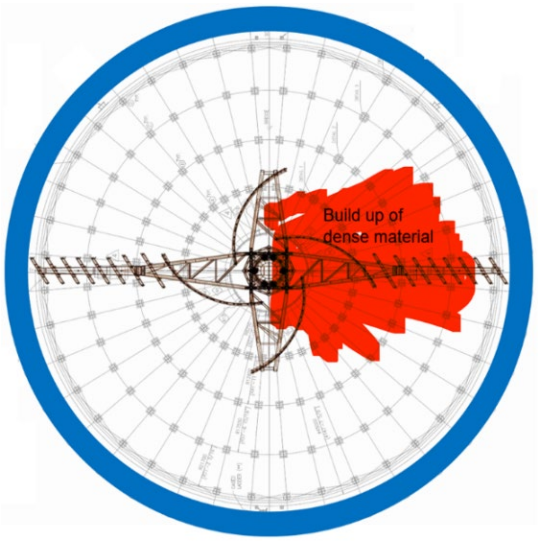

Figure 1 Build-up of thick bed material

Upset loads are particularly critical in high-density thickening applications, where the rheological resistance of settled solids can increase abruptly and nonlinearly. Although feedwell designs aim to promote uniform solids distribution and rake mechanisms are engineered for comprehensive coverage, real-world operations are inherently variable. Fluctuations in feed composition, flocculant dosage, sedimentation behaviour, and control system responsiveness can all contribute to uneven solids build-up and localised resistance zones. These effects are especially pronounced in paste and deep-cone thickeners, where underflow yield stresses routinely exceed 100 Pa (Ruan et al. 2019).

Such conditions may trigger abrupt torque spikes and mechanical instability, often initiated by process disturbances such as feed surges, flocculant overdosing, or control system lag. These disturbances can induce sediment sloughing and the formation of dense deposits in isolated regions of the thickener floor – areas that may lie inside the rake's routine engagement path. When encountered, these deposits impose concentrated resistance loads far beyond the normal operating envelope.

Mechanically, upset loads differ fundamentally from normal loads. Normal loads are continuous, predictable, and broadly distributed across the rake structure, whereas upset loads are transient, spatially concentrated, and frequently exceed design thresholds. Their magnitude and location are inherently difficult to predict, making them a major source of uncertainty in thickener design and operation. If not properly accounted for, upset loads can precipitate drive overloads, structural cracking, or catastrophic component failure – particularly in systems operating near torque or stress limits.

Given their potential to compromise system integrity and halt production, upset loads must be treated as primary design constraints, rather than secondary operational contingencies. They directly influence the torque rating of the drive system, the structural robustness of rake components, and the logic of overload protection systems. Despite their significance, upset loads have received limited attention in the open literature. Most published studies focus on normal rake loads under idealised conditions, leaving a critical gap in understanding the dynamic, localised, and failure-inducing nature of upset events.

This study addresses that gap by applying a high-fidelity FSI methodology to quantify upset loads under realistic field scenarios. The results provide new insight into the mechanical demands imposed by sediment island formation and other non-uniform loading phenomena, offering a more robust foundation for the design and operation of modern thickening systems.

2.3 Rake-load quantification

Accurate quantification of rake loads is essential for the design of reliable and efficient thickener systems. CFD has emerged as a powerful tool in this regard, providing a physics-based framework to predict hydraulic interactions within the thickener. Under normal operating conditions, CFD enables detailed evaluation of flow behaviour, pressure distributions, and shear stresses acting on rake blades and arm surfaces. Early studies by Frost et al. (1993), Sutalo et al. (2003), and Rudman et al. (2008) demonstrated the utility of CFD in modelling steady-state behaviour, estimating torque requirements, and assessing energy consumption in laboratory- and pilot-scale thickeners. These efforts established a foundation for understanding how rake geometry, rotational speed, and slurry rheology influence mechanical loading during routine operation.

Despite these advances, most published CFD analyses have been limited to small-scale thickeners, where boundary conditions, feed properties, and sediment profiles can be tightly controlled. While such simulations yield valuable insights, they do not fully capture the complexity and variability inherent in full-scale industrial systems – particularly deep-cone thickeners used for tailings dewatering. In these systems, mud beds are deeper, solids concentrations are higher, and rheological behaviour is both anisotropic and nonlinear, making direct extrapolation from pilot-scale data unreliable.

Unlike normal rake loads, which can often be estimated using steady-state simulations and isotropic rheology models, upset rake loads are inherently transient and stochastic. Their occurrence depends on a dynamic interplay of process conditions, local material properties, and equipment response – including sediment consolidation, rake geometry, rotational speed, and hydraulic resistance. Quantifying these loads requires

advanced simulation techniques capable of resolving time-dependent interactions and localised concentration effects.

To address this challenge, FSI approach has been proposed as a promising methodology. By coupling transient multiphase CFD with FEA, FSI enables seamless integration of hydraulic load predictions with structural response analysis. The only known FSI-based study of a full-scale thickener was presented at the 2024 SME Annual Conference (Lu et al. 2024), demonstrating the feasibility of simulating rake loads under realistic industrial conditions. That pioneering work, however, focused primarily on normal load scenarios, leaving the quantification of upset loads – those arising from sediment island formation, torque spikes, and flow disruptions – an open research frontier.

This study seeks to bridge that gap by developing a comprehensive framework to quantify both normal and upset rake loads in a full-scale deep-cone thickener. Through the integration of CFD modelling, field instrumentation, rheological characterisation, and structural analysis, the proposed methodology captures the full spectrum of rake loading conditions – from steady-state operation to transient overload events. The ultimate objective is to enhance mechanical reliability, reduce operational risk, and support the development of next-generation thickener technologies with predictive control capabilities tailored to high-density paste environments.

3 Process description

Figure 2 shows the overall configuration of the raked thickener evaluated in this study: an FLSmidth 45-metre deep-cone thickener, currently recognised as the largest operational unit of its kind worldwide. Engineered for high-throughput copper tailings dewatering, this thickener is designed to deliver an underflow concentration of up to 68 wt%, supporting downstream paste handling and water recovery objectives.

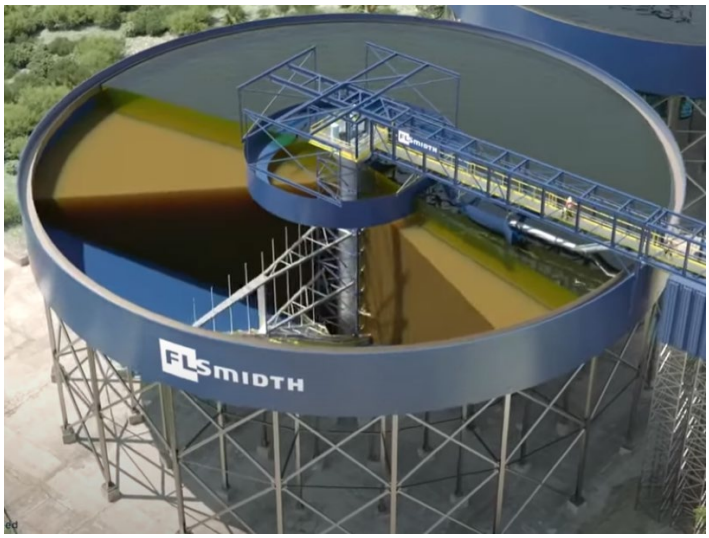

Figure 2 Configuration of typical raked thickener

The rake mechanism features a four-arm assembly, each outfitted with FLSmidth's patented inner spiral blade technology, which enhances solids mobilisation and bed conditioning. The rake is powered by a hydraulic drive system, selected for its ability to deliver high torque at low rotational speeds under demanding rheological conditions. The short-arm assembly spans a diameter of approximately 19.5 m, and the system operates at a nominal rake speed of 0.075 RPM, consistent with industry standards for deep-cone applications. This configuration reflects a modern approach to thickener design, integrating advanced blade geometry, high-density underflow capability, and robust mechanical drive systems. The deep-cone profile promotes enhanced sediment consolidation, while the spiral rake blades improve solids transport efficiency and reduce the risk of localised build-up.

Its typical feed conditions for this thickener – including flow rate, solids concentration, flocculant dosage, and rheological properties – are summarised in Table 1. These parameters were used to initialise the CFD simulations and inform the FEA model inputs, ensuring that the fluid–structure interaction analysis reflects realistic operational scenarios. The selected configuration and process conditions provide a representative basis for evaluating both normal and upset rake loads in high-density thickeners.

Table 1 Typical feed conditions

Parameters	Value
Solid content (wt%)	31–36
Solid rate (t/h)	1,120
Undiluted rate (m^3/h)	2,835
Diluted rate (m^3/h)	8,613

3.1 Island location

To replicate field observations, it is postulated that a dense material unexpectedly settles onto a localised area of the floor bed, resulting in the formation of a mud island. While such islands may exhibit various geometries, a hemispherical shape is adopted for modelling simplicity, with its centre positioned directly on the inner surface of the floor bed. To represent a worst-case scenario, it is further assumed that all solids carried in the feed stream contribute to the island's build-up. Due to the distinct raking patterns of the short and long arms, 2 plausible deposition zones are identified – termed the inner island and outer island, respectively.

3.1.1 Inner island

When all solids settle within the reach of the short-arm mechanism (radius R = 9.75 m), both the short-arm and long-arm rakes are capable of accessing and scraping the region. Under this condition, the time interval between 2 successive raking actions is approximately 200 seconds. As a result, an inner island forms with a total volume of 33 m^3, geometrically represented as a hemispherical deposit with a radius of 2.5 m, as illustrated in Figure 3.

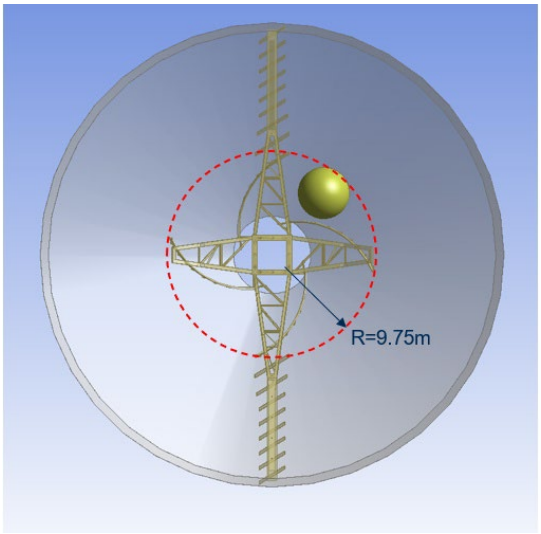

Figure 3 Inner island

3.1.2 Outer island

If solids accumulate beyond the short-arm's effective radius (R = 9.75 m), the short-arm rake cannot reach the deposit, leaving only the long-arm rake to perform scraping operations. In this case, the interval between successive raking actions increases to approximately 400 seconds. Consequently, an outer island develops with a total volume of 66.9 m³, corresponding to a hemispherical shape with a radius of 3.2 m, as shown in Figure 4.

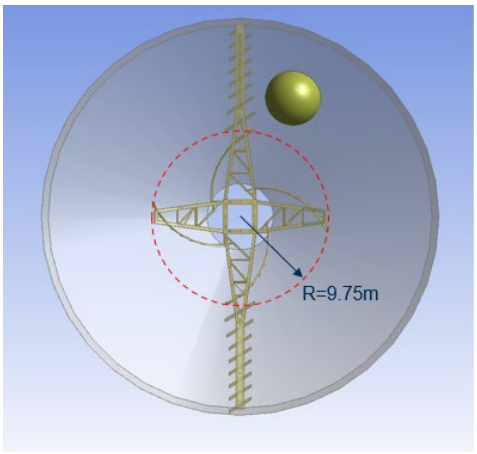

Figure 4 Outer island

3.2 Island material

With a lack of material property from a real island formed in field thickeners, a semisolid paste with a yield stress of 400 Pa, as shown in Figure 5, is assumed. The rest of the thickener tank volume will be filled by the normal bed-mud sediment with the rheology parameters given in Table 2 and flow curves in Figure 5.

Table 2 Rheology of normal bed mud and island materials

Property	Normal bed mud	Island material
Density (kg/m³)	1,765	1,950
Yield stress (Pa)	13.85	400
Flow consistency index	0.1	100
Flow behaviour index	1	1

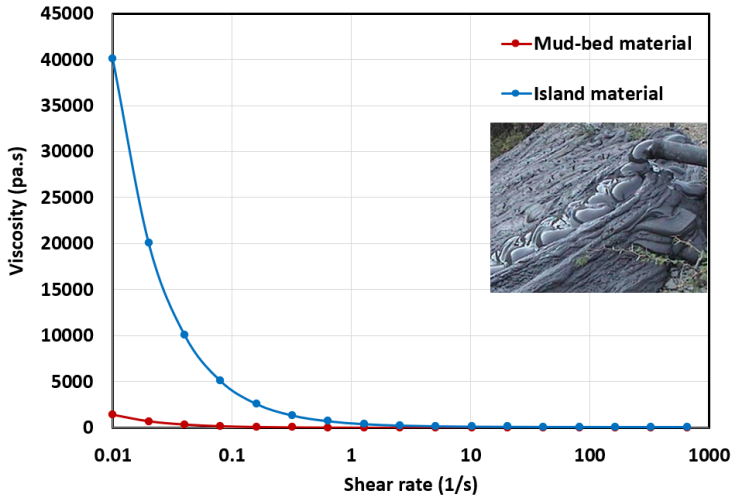

Figure 5 Rheology of mud bed and island materials

3.3 Rake material

It is further assumed that the rake and associated structures were made of the same steel with mechanical properties given in Table 3.

Table 3 Mechanical properties of associated rake structures

Parameter	Value
Elastic modulus	200 GPa
Poisson's ratio	0.26
Shear modulus	79.3 GPa
Tensile strength	400 MPa
Yield strength	315 MPa

4 Fluid–structure interaction analysis

In the design and analysis of rake systems, accurate quantification of hydrodynamic loads is essential to ensure both mechanical integrity and operational reliability. Conventional CFD simulations typically provide integrated force components (Fx, Fy, Fz) and torque components (Tx, Ty, Tz) acting on the rake assembly. While these global outputs are informative, their direct application to structural design introduces ambiguity – particularly when redistributing CFD-derived loads across complex rake geometries for FEA. Without a robust load-transfer methodology, significant uncertainty can arise in stress evaluation, fatigue assessment, and material selection.

To address this challenge, this study introduces a one-way FSI framework tailored for mineral processing equipment as shown in Figure 6. The fluid domain is resolved using the Ansys Fluent solver, capturing transient flow behaviour and particle-laden slurry dynamics of high-density paste environments. Once convergence is achieved, pressure and shear loads are mapped directly onto the rake and arm surfaces of a coupled structural model in Ansys Mechanical. This mapping is performed at the computational cell level, preserving spatial fidelity and eliminating the need for manual load redistribution or empirical approximations.

By enabling direct transfer of transient fluid loads to the structural mesh, the one-way FSI approach facilitates accurate stress and deformation analysis under realistic operating conditions. Integrating solver outputs across disciplines enhances confidence in design decisions, supporting optimisation of blade geometry, arm sizing, and material durability. This methodology is particularly advantageous for deep-cone thickeners and other high-torque applications, where conventional design heuristics often prove inadequate.

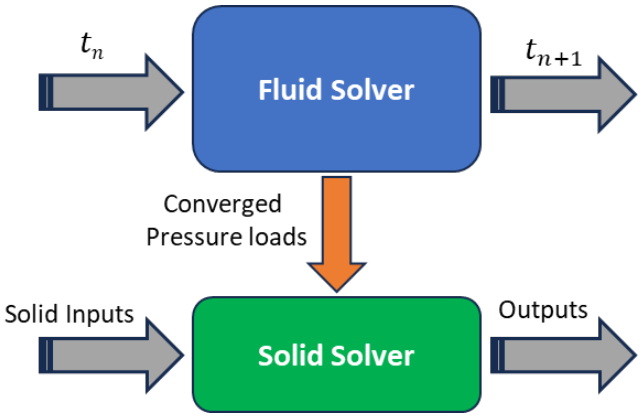

Figure 6 One-way fluid–structure interaction workflow

4.1 Computational fluid dynamics solution

4.1.1 Inner island

Figure 7 illustrates the morphological evolution of the inner island before (t = 0 s) and after (t = 200 s) the raking operation. The simulation captures the progressive disintegration of the island structure under the combined influence of the short and long rake arms. This dual-action mechanism effectively mobilises and transports the majority of the consolidated material toward the underflow discharge zone, thereby restoring flow continuity and improving solids removal efficiency.

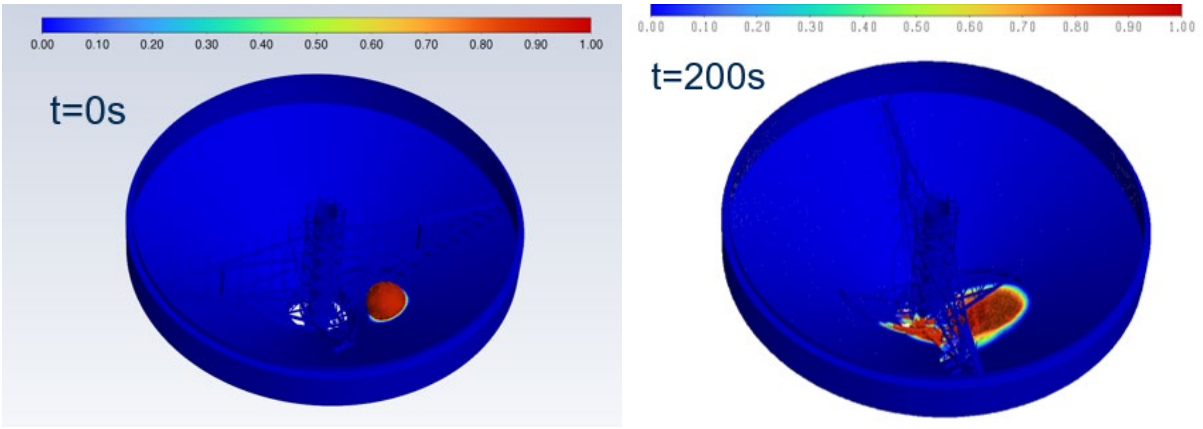

Figure 7 Inner island location and shape before and after raking action

Figure 8 presents the time-resolved profiles of rake torque components (Tx, Ty, Tz) and force components (Fx, Fy, Fz) throughout the raking cycle. Among these, the rotational torque about the rake shaft axis (Ty) exhibits a pronounced transient spike, reaching a peak of 240,699 N·m at approximately t = 80 s. This sharp increase corresponds to the rake engaging and penetrating the dense inner island mass, which imposes substantial resistance to rotation. By contrast, the remaining torque and force components remain relatively stable and low in magnitude, indicating that the primary mechanical challenge during island breakup is concentrated in the rotational domain.

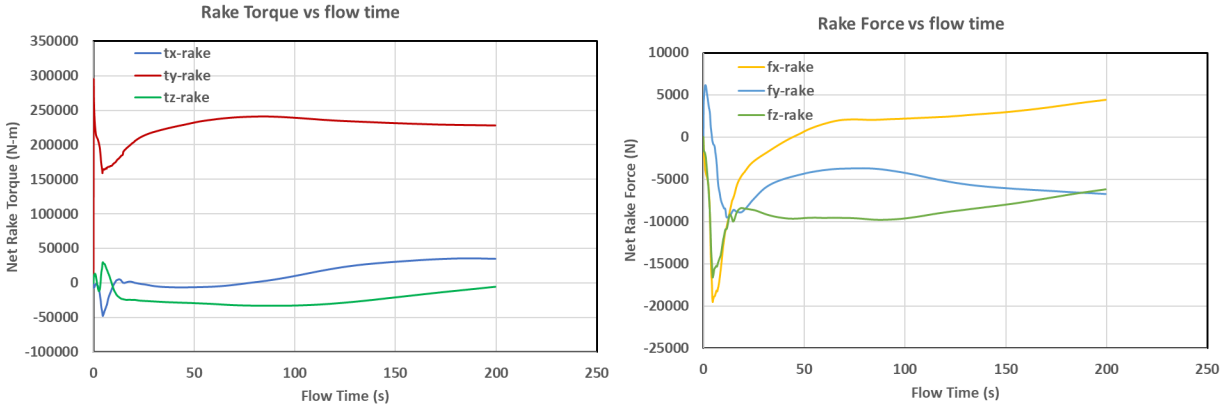

Figure 8 Torque and force profile during inner island breakup

This behaviour underscores a critical design consideration: upset loads induced by inner island collapse manifest predominantly as short-duration torque surges rather than as broadly distributed structural loads. These findings are consistent with field observations from high-density thickener operations, where sudden torque excursions are frequently recorded during island breakthrough events. The simulation results therefore provide a valuable predictive tool for anticipating peak torque demands and guiding the design of rake drive systems, torque limiters, and structural reinforcements.

4.1.2 Outer island

Figure 9 illustrates the morphological evolution of the outer island before (t = 0 s) and after (t = 200 s) the raking operation. Unlike the inner island scenario, only the long rake arm is able to reach the outer island, resulting in a single-point raking action. Consequently, a smaller volume of consolidated material is mobilised, and the overall scraping efficiency is reduced.

Figure 10 presents the transient profiles of rake torque (Tx, Ty, Tz) and force (Fx, Fy, Fz) components during the raking process. Two significant torque spikes are observed: a peak rotational torque (Ty) of 366,951 N·m at t = 40 s, and a peak lateral torque (Tx) of 180,000 N·m at t = 150 s. Compared with the inner island case, the elevated Ty response is attributed to the larger mass of outer island material and its greater radial distance from the rake's rotational centre, which amplifies the moment arm and resistance during engagement.

The pronounced Ty spike represents a critical upset load that may cause drive system overloading, torque limiter activation, or rake stalling – phenomena frequently reported in field operations. In addition, the elevated Tx torque and associated force components (Fx, Fy, Fz) indicate asymmetric loading conditions. These unbalanced forces can induce lateral displacement of the rake assembly, potentially leading to misalignment, mechanical interference with tank internals, or collision with structural boundaries.

Taken together, the outer island scenario introduces a dual-mode risk profile: rotational torque overload (Ty) and lateral instability due to unbalanced loads (Tx, Fx, Fy, Fz). These findings highlight the importance of incorporating transient load predictions into rake design and control strategies, particularly for deep-cone thickeners and high-density paste applications. The simulation results provide valuable insight into potential failure modes and support the development of mitigation measures such as reinforced rake arms, adaptive torque control, and predictive maintenance protocols.

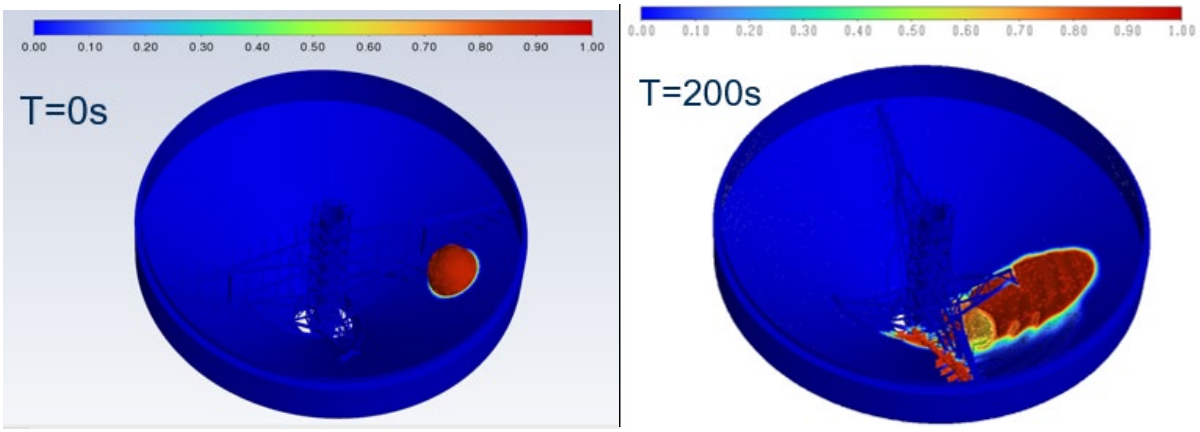

Figure 9 Outer island location and shape before and after raking action

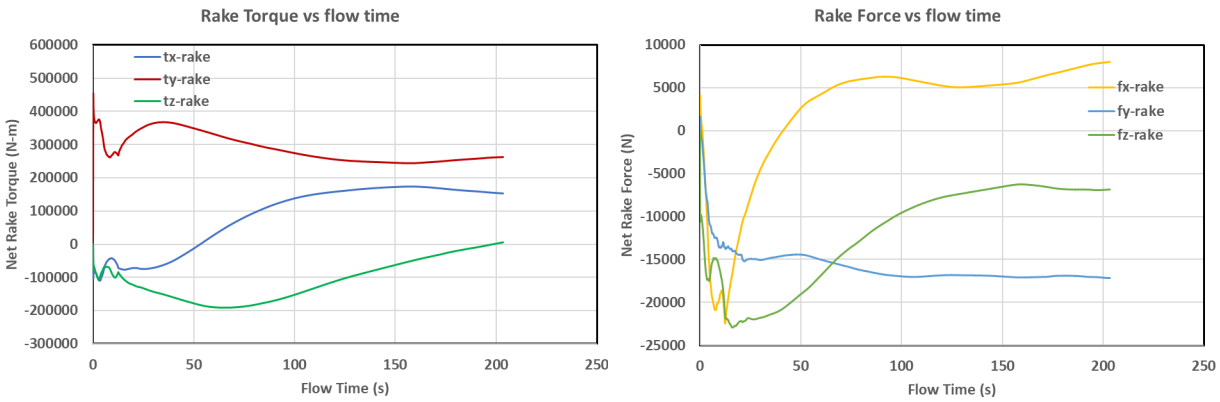

Figure 10 Torque and force profile during outer island breakup

4.1.3 Comparison

To evaluate the relative impact of island-induced upset loads on rake performance, a baseline simulation was conducted under identical operating conditions but without the presence of island structures. This normal load scenario represents the steady-state behaviour of the rake interacting solely with a uniform mud bed, absent localised consolidation.

Figure 11 compares the pressure distributions generated for 3 scenarios: the normal mud bed, the inner island, and the outer island. These visualisations highlight the localised pressure intensification associated with island formation, particularly near the rake-blade interfaces. Figure 12 further quantifies the mechanical response by comparing predicted rake loads – both torque and force components – under normal and upset conditions.

The results show that the inner island induces a 23% increase in rotational torque and a 194% increase in total force relative to the normal condition. In contrast, the outer island produces an 88% increase in rotational torque and a 593% increase in total force. These elevated load profiles underscore the disruptive influence of island formation, particularly in high-density paste environments where material consolidation is prevalent.

The surge in rotational torque (primarily Ty) emerges as a critical factor contributing to drive system overloading, torque spikes, and potential activation of torque limiters. Meanwhile, the substantial increases in force components (Fx, Fy, Fz) reflect asymmetric loading conditions that can lead to rake misalignment, mechanical interference, and blockage events. These findings align closely with field observations, where sudden torque excursions and rake jamming are frequently reported during island breakthrough phases.

By benchmarking upset loads against normal operating conditions, this study establishes a quantitative framework for risk assessment and mitigation. The insights gained support the development of more resilient rake systems, including torque-tolerant drive units, adaptive control algorithms, and predictive maintenance protocols tailored to thickener operations prone to island formation.

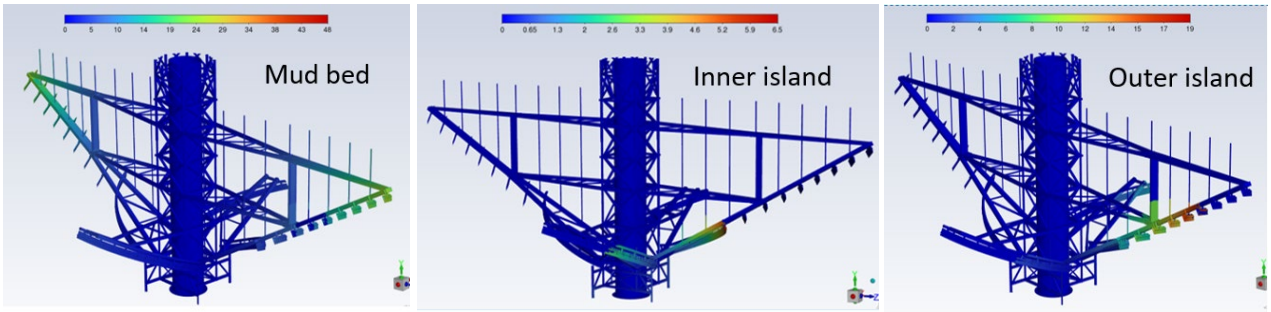

Figure 11 Compared raking pressure – mud bed versus inner versus outer island

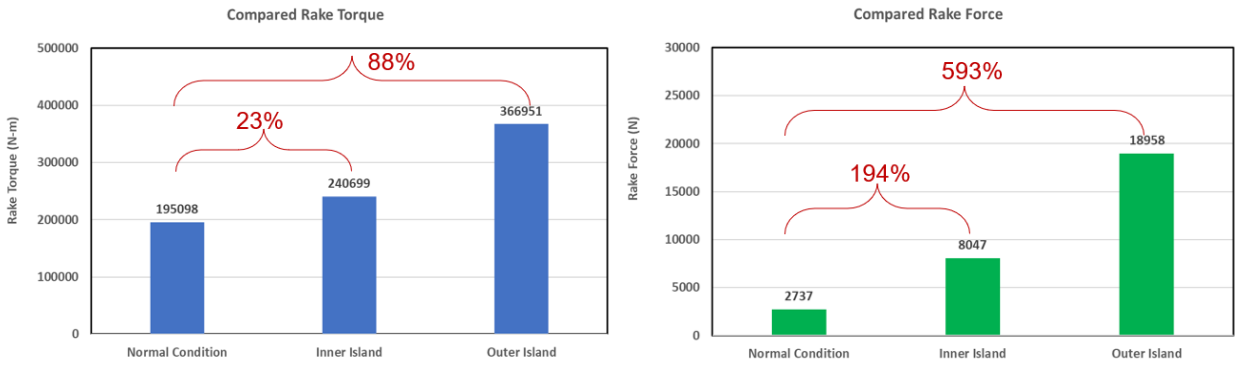

Figure 12 Compared upset loads versus normal loads – inner versus outer Island

4.2 Finite element analysis solution

4.2.1 Inner island

To evaluate the structural integrity of the rake system under island-induced loading, the CFD-predicted pressure and shear-stress fields were mapped onto the coupled surfaces of the FEA model. Figure 13 illustrates the resulting pressure distributions, incorporating both hydrostatic pressure from the mud-bed slurry and pressure contributions from rake motion under normal and upset loading conditions. These mapped loads capture the transient fluid–structure interactions that occur during rake engagement with the inner island. To better approximate field conditions, simplified top blocks were incorporated into the FEA model to represent pre-stress effects imposed by the surrounding enclosure and bridge structures. This addition ensures that the structural response accounts for external constraints commonly present in thickener installations.

Figure 14 presents the total deformation and von Mises stress contours obtained from the FEA simulation. The analysis indicates that both deformation and stress levels remain within acceptable limits under the evaluated loading conditions. Specifically, the peak deformation reaches 6.47 mm, while the maximum stress is 65.3 MPa – well below the typical yield thresholds of structural steels used in rake assemblies. These results suggest that, despite the transient upset loads associated with inner island breakup, the rake structure maintains mechanical stability without experiencing excessive strain or displacement.

The validated FEA framework thus provides a reliable foundation for future design optimisation, including material selection, weld reinforcement, and fatigue life assessment under intermittent torque spikes and slurry-induced pressure surges.

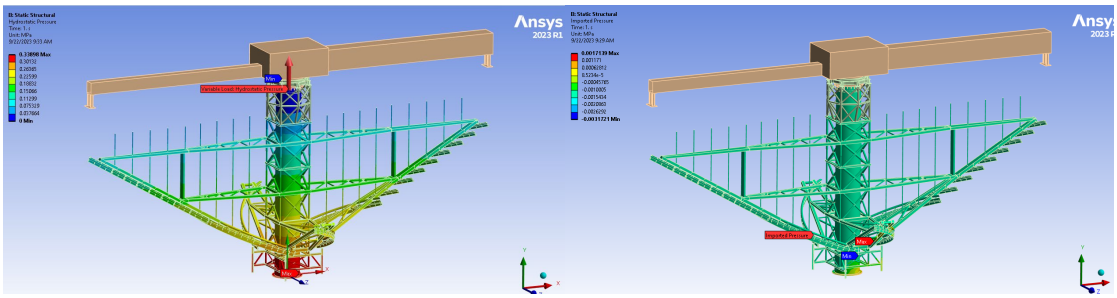

Figure 13 Hydrostatic pressure and pressure mapped from computational fluid dynamics – inner island

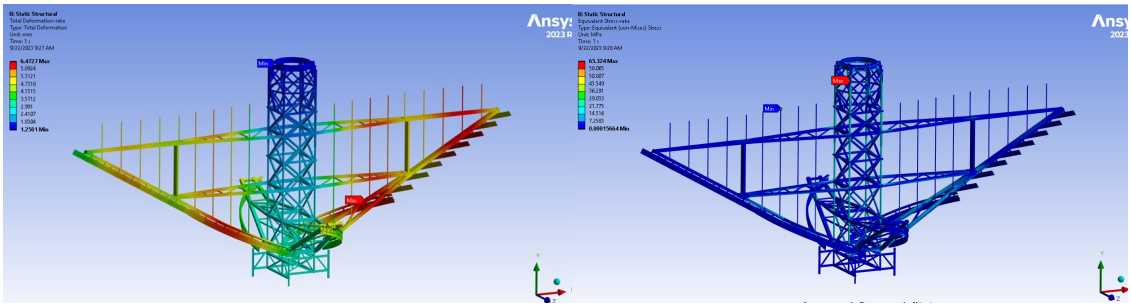

Figure 14 Total deformation and stress response – inner island

4.2.2 Outer island

To assess the structural impact of upset loads generated by outer island formation, the hydrodynamic loads obtained from the CFD simulation were mapped onto the corresponding surfaces of the FEA model. Figure 15 illustrates the combined pressure distribution, incorporating both baseline hydrostatic pressure from the mud bed and dynamic pressure contributions arising from rake interaction with the outer island. These mapped loads capture the transient fluid–structure interaction and highlight the localised intensification of pressure near the rake-blade interface. As in the inner island scenario, simplified top blocks were included in

the FEA model to represent pre-stress effects imposed by surrounding bridge and enclosure structures, thereby ensuring that external constraints typical of thickener installations were accounted for.

Figure 16 presents the resulting total deformation and von Mises stress contours. The analysis indicates a peak deformation of 6.39 mm and a maximum stress of 65.7 MPa – both of which remain within acceptable limits for standard structural steels commonly used in rake assemblies. These results suggest that, despite the elevated and asymmetric loading conditions associated with outer island engagement, the rake structure retains mechanical stability without exceeding critical stress thresholds.

However, when considered alongside the torque and force spikes identified in the CFD solution, the outer island scenario represents a higher risk of mechanical upset compared with the inner island case. The combination of increased radial loading and unbalanced force vectors may contribute to rake misalignment, drive system overload, and potential collision with tank internals. The validated FEA framework therefore provides a critical insight for identifying structural vulnerabilities and guiding design improvements – such as reinforced rake arms, optimised blade geometry, and adaptive torque control systems – to mitigate risks associated with island-induced upset events.

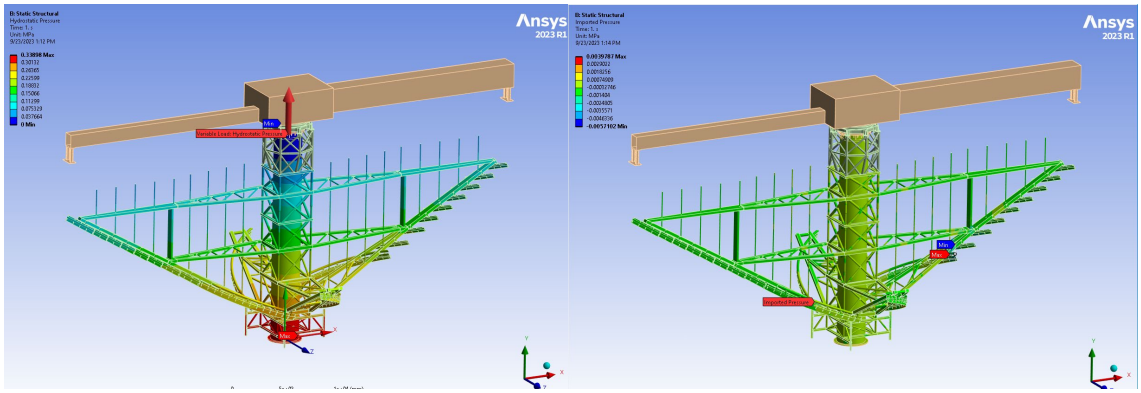

Figure 15 Hydrostatic pressure and pressure mapped from computational fluid dynamics – outer island

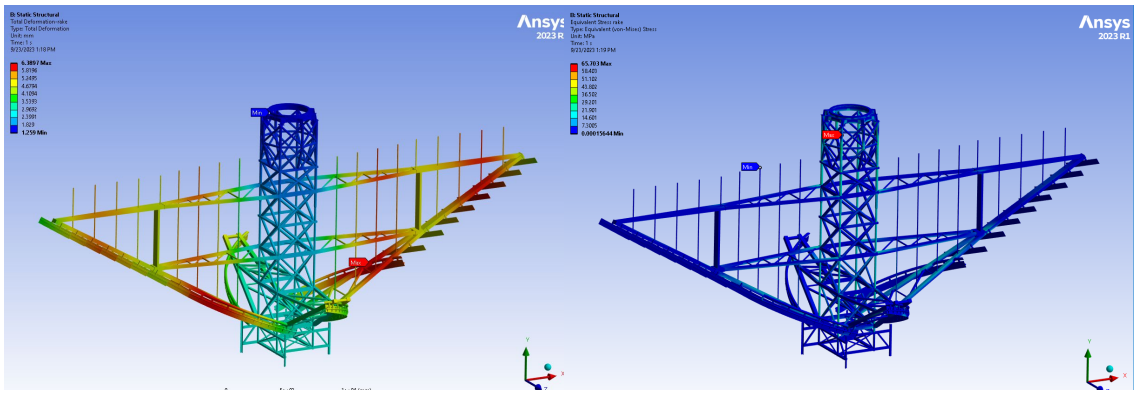

Figure 16 Total deformation and stress response – outer island

4.2.3 Comparison

To evaluate the structural implications of island-induced upset loads, Table 4 summarises the FEA results for both inner and outer island scenarios. These results are benchmarked against the material yield stress of 315 MPa specified in Table 3. In both cases, the observed peak stress remains well below the design tolerance, with a maximum of approximately 65 MPa, confirming that the rake structure operates safely within its elastic range under the evaluated upset conditions.

Despite the substantial increases in rake torque and force documented in Figure 12 – where inner island formation produces a 23% increase in torque and a 194% increase in force, and outer island formation results in an 88% increase in torque and a 593% increase in force – the structural response reported in Table 4 does

not exhibit a proportionally amplified deformation or stress outcome. This apparent discrepancy arises from the nature of the FEA outputs, which reflect the cumulative effect of all applied loads, including hydrostatic pressure, vertical slurry resistance, and mapped CFD pressure fields.

Within the context of total loading, the upset contributions from island formation – though significant in terms of transient torque and lateral force spikes – represent only a fraction of the overall structural demand. Vertical loads dominate the stress and deformation response due to the rake's orientation and support configuration, thereby diluting the influence of lateral upset forces in the global metrics.

These results show that although island-induced upset loads do not present an immediate structural-strength concern for the rake, they remain operationally significant. The associated torque and force excursions can trigger drive overload, induce rake misalignment, and cause mechanical interference – issues commonly reported in field operations. Consequently, structural robustness must be paired with resilient mechanical design and control measures, including torque-limiting devices, adaptive drive systems, and predictive maintenance strategies, to ensure safe and reliable thickener performance under upset conditions.

Table 4 Structural response under upset loads caused by inner and outer islands

Structure response	Inner island t = 80 s	Outer island t = 40 s
Total deformation (mm)	6.47	6.39
Max stress (MPa)	65.3	65.7

5 Conclusion

This study applied a high-fidelity, one-way FSI framework to quantify transient upset loads arising from localised material build-up in a 45 m industrial raked thickener. Two field-relevant worst-case scenarios – inner island and outer island formation – were evaluated through coupled transient CFD and structural FEA analyses.

The CFD results show that outer-island formation produces the most severe hydraulic loading, generating a peak torque of approximately 366,951 N·m (an 88% increase over baseline) due to the larger consolidated mass and extended radial moment arm. Inner-island formation, while less extreme, still induced a 23% torque increase. Both scenarios produced substantial asymmetric force amplification, with lateral force components increasing by up to 593%, highlighting the role of non-rotational load vectors (Tx, Fx, Fy, Fz) in driving rake misalignment, drive overload, and mechanical interference with tank internals.

Structural FEA confirmed that, despite these large transient loads, the rake structure remains within safe limits. Maximum deformation (6.5 mm) and peak stress (<66 MPa) were well below the material yield strength (315 MPa), indicating that acute structural failure is unlikely under isolated upset events. Instead, operational vulnerability is more strongly linked to drive-unit torque capacity and the system's ability to accommodate unbalanced lateral loading.

Overall, the results validate the effectiveness of the one-way FSI methodology as a predictive tool for quantifying upset loads in raked thickeners. With continued refinement and validation, this framework can support the design of torque-tolerant drive systems, improved lateral bracing strategies, and adaptive control algorithms, ultimately enhancing reliability and performance in high-density paste applications where island formation is prevalent.

References

Albertson, OE & Okey, RW 1992, 'Evaluating scraper designs', *Water Environment Technology*, vol. 4, no. 1, pp. 52–58.

Frost, RC, Halliday, J & Dee, AS 1993, 'Continuous consolidation of sludge in large scale gravity thickeners', *Water Science & Technology*, vol. 28, pp. 77–86.

Gollaher, T, Johnson, JL, Biesinger, MT & Accioly, AHL 2010, 'Paste thickening tailings – recent examples of a rapidly emerging technology', *Proceedings of the SME Annual Conference*, Society for Mining, Metallurgy & Exploration, Englewood.

Gunthert, FW 1984, 'Thickening zone and sludge removal in circular final settling tanks', *Water Science & Technology*, vol. 16, no. 10–11, pp. 303–316, https://doi.org/10.2166/wst.1984.0232

Hazen, A 1904, 'On sedimentation', *Transactions of the American Society of Civil Engineers*, vol. 53, no. 2, pp. 45–71, https://doi.org/10.1061/TACEAT.0001655

Lu, YJ, Sok, T, Schoenbrunn, F, Scott, J & Gilbert, C 2024, 'FSI analysis of mud-rake Interaction in a full-scaled thickener', *Proceedings of the SME Annual Conference*, Society for Mining, Metallurgy & Exploration, Englewood.

McCarty, MF & Olson, R 1959, 'Polyacrylamides for the Mining Industry', *Mining Engineering*, vol. 11, no. 1, pp. 61–65.

Ruan, Z, Wang, Y, Wu, AX, Yin, SH & Jin, F 2019, 'A theoretical model for the rake blockage mitigation in deep cone thickener: a case study of lead-zinc mine in China', *Mathematical Problems in Engineering*, vol. 11, pp. 1–7, https://doi.org/10.1155/2019/2130617

Rudman, M, Paterson, DA & Simic, K 2008, 'Raking in gravity thickeners', *International Journal of Mineral Processing*, vol. 86, no. 1–4, pp. 114–130, https://doi.org/10.1016/j.minpro.2007.12.002

Rudman, M, Paterson, DA & Simic, K 2010, 'Efficiency of raking in gravity thickeners', *International Journal of Mineral Processing*, vol. 95, no. 1, pp. 30–39, https://doi.org/10.1016/j.minpro.2010.03.007

Schoenbrunn, F 2011, 'Dewatering to higher densities - an industry review', in R Jewell & AB Fourie (eds), *Paste 2011: Proceedings of the 14th International Seminar on Paste and Thickened Tailings*, Australian Centre for Geomechanics, Perth, pp. 19–23, https://doi.org/10.36487/ACG_rep/1104_02_Schoenbrunn

Sutalo, ID, Paterson, DA & Rudman, M 2003, 'Flow visualization and computational prediction in thickener rake models', *Minerals Engineering*, vol. 16, no. 2, pp. 93–102, https://doi.org/10.1016/S0892-6875(02)00256-X

Warden, JH 1981, 'The design of rakes for continuous thickeners. Especially for waterworks coagulant sludges', *Filtration Separation*, vol. 18, no. 2, pp. 113–116.